



Gas Flow and Heat Transfer in an Enclosure Induced by a Sinusoidal Temperature

J. Baliti^{1†}, M. Hssikou² and M. Alaoui³

¹ Polydisciplinary Faculty, Sultan Moulay Slimane University, Beni Mellal – Morocco

² Faculty of Sciences, Ibn Zohr University, Agadir – Morocco

³ Faculty of Sciences, Moulay Ismail University, Meknes – Morocco

†Corresponding Author Email: (j.baliti@edu.umi.ac.ma)

(Received June 23, 2018; accepted January 27, 2019)

ABSTRACT

The heat transfer and flow characteristics of rarefied gas confined within a square cavity are investigated. The cavity upper-wall is subjected to a symmetrical sinusoidal temperature with respect to its midline. Two cases are considered, one of them is that the bottom and two sidewalls are kept adiabatic, while in the other, all the enclosure walls are considered diffusely reflecting. Kinetically, the gas is simulated with the direct simulation Monte Carlo method (DSMC) in the slip and transition regimes. The DSMC results are compared with the Navier-Stokes-Fourier equation, with second order boundary conditions of velocity slip and temperature jump, (NSF) in the slip regime. Main outcomes are presented as velocity streamlines overlaid on temperature contours and macroscopic parameters plots. The Knudsen number (Kn) increase shows other vortices, beside the two classical ones that appear in the hydrodynamic and slip regime. The normal heat flux about the sinusoidally heated wall is strengthened by the flow in DSMC rather than that predicted by NSF method. Good agreement is observed between the NSF theory and DSMC method in the early slip regime, but when $Kn=0.1$ the NSF approach breaks down to show the secondary counter rotating eddies illustrated by the DSMC method.

Keywords: DSMC; NSF; Heat transfer; Sinusoidal temperature.

1. INTRODUCTION

A good understanding of fluid mechanics at the micro-scales is important to get a better insight of the microfluidic process, which can lead to the development of more efficient microsystems (Karniadakis *et al.*, 2006; Baliti *et al.*, 2017). The experiments in pressure microsensors have shown that the classical continuum theory of gas dynamics (i.e. the Euler and Navier-Stokes-Fourier equations) cannot explain the behavior of gas flow under these conditions. The thermal behavior of gas flow in microcavities, commonly used as a benchmark configuration, is usually affected by many non-equilibrium phenomena, such thermal slip and heat transfer without temperature gradient (Hssikou *et al.* 2016a). To understand the physics of such systems, kinetic or extended macroscopic description is needed (Baliti *et al.*, 2018a). A revolution in understanding and utilizing micromechanical devices is starting since last decades. The utility of these devices will be enormous, and with time, they will fill the niches of our lives pervasively as

electronics (Karniadakis *et al.*, 2006; Gad-el-Hak, 2001). Great attention has been directed in recent years to the microelectromechanical systems (MEMS), owing to their advantages over their macro homologues, such as the relatively lower expense for manufacture in large quantities, the small size and mass rendering them possible to fit in specific situations, and the quick reaction from their minimal inertia, etc. The manufacturer of a MEMS device needs to understand the relation between the processing and the properties of the material (Islam, 2012). However, the prediction of the flow properties and heat transfer characteristics in the microdevices has not developed at the same rapid cadence as micro fabrication techniques. The Industrial motivation of paper is to understand the heat transfer characteristics in glass melting tanks, where a number of burners placed above the glass tank create periodic temperature profiles on the surface of the glass melt; see (Sarris *et al.*, 1999; Jian *et al.*, 2000). Currently, since MEMS can be manufactured in micron size, it becomes possible for the gaseous flow to possess a mean free path comparable to the characteristic length of the device

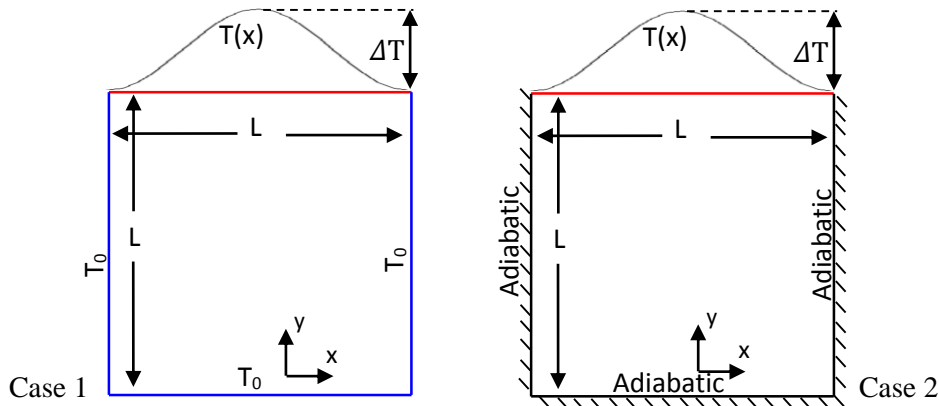


Fig. 1. Schematic illustration of the system geometry.

even at standard conditions (Le, 2011). In accordance with the ratio of the mean free path over the length of the micro device, called the Knudsen number (Kn), one can differentiate between four main flow regimes, and looks on the appropriate method to analyze the flow of gases. Basing on this dimensionless quantity, the flow is considered in the continuum regime when $Kn < 0.001$. The slip regime is reached when the Knudsen number is in the range of $0.001 \leq Kn < 0.1$. Beyond that, the transition flow regime begins ($0.1 \leq Kn < 10$). When the Knudsen number is sufficiently higher ($Kn \geq 10$), the free molecular regime, the gas particles move more freely (Karniadakis *et al.* 2006; Gad-el-Hak, 2001; Struchtrup & Taheri, 2011).

The dimensions of the MEMS devices determine the regime where the flow lie in. The micro systems cover the continuum, slip and early transitional flow regimes. Further miniaturization of MEMS device components and nanotechnology applications correspond to higher Knudsen numbers, making it necessary to study the mass, momentum and energy transport in the entire Knudsen regime (Karniadakis *et al.*, 2006; Beskok, 2001). The continuum approach, given by the Navier-Stokes and Fourier equations (NSF), is only valid and perfectly describes the flow in the hydrodynamic regime. In the slip regime, the continuum assumption still valid but with specific boundary conditions of velocity slip and temperature jump at boundaries (Karniadakis *et al.*, 2006; Gad-el-Hak, 2001). As the Knudsen number increases, rarefaction effects become more important, and ultimately the continuum approach breaks down altogether. In the transition flow regime, the mean free path for a gas becomes comparable to a characteristic length of the micro system. In this regime, the flow is described by the Boltzmann equation (Cercignani & Gabetta, 2007; Chapman & Cowling, 1970), but cannot be easily solved. Consequently, alternative solutions are needed, like the direct simulation Monte Carlo method (DSMC) developed by Bird (Bird, 1994, 1976] which is valid for all ranges of Knudsen number, though it is computationally expensive. Other alternative approaches like molecular-based

models (Shakhov, BGK...) or macroscopic equations of high moments (Grad 13 moments, R13...) are widely used. In the free-molecular flow regime, the nonlinear collision integral is negligible, and the Boltzmann equation is drastically simplified. Analytical solutions are possible in this case for simple geometries and numerical integration of the Boltzmann equation, which is straightforward for arbitrary geometries. It provided that the surface-reflection characteristics are accurately modeled (Karniadakis *et al.* 2006; Gad-el-Hak, 2001).

In the present study, we lean on the analysis of the flow and heat transfer rarefied gas confined within a square enclosure. The work investigates the non-equilibrium gas flows encountered especially in the vacuum and micro-devices systems. The thermal behavior of such flows is strongly related to the flow rarefaction degree which defines the heat transfer mode. Unlike almost of previous study, which concerns the convection heat transfer process in continuum gas flows, in this paper we focus on the rarefaction effects on heat transfer gas flow in a periodically heated cavity. The non-equilibrium is conducted by a sinusoidal temperature profile applied along the top wall. Using both kinetic (DSMC) and macroscopic (NSF) approaches, two cases are investigated differing in their boundaries type. The first is related to the whole walls which are diffusely reflecting, while three walls, the bottom and sidewalls, are adiabatic in the second.

2. PROBLEM STATEMENT

The treated problem is an enclosure filled with a monatomic rarefied gas. The square cavity is taken for the first case (Case 1) to have the upper wall heated by a sinusoidal temperature $T(x)$ (Equation 1), while the three others are diffuse reflecting taken to the environmental temperature T_0 .

The second case (Case 2) differs from the first by the three adiabatic walls, instead of the diffuse ones in the first (Fig.1). The sinusoidal temperature distribution $T(x)$ which is applied on the top wall reads:

$$T(x) = T_0 + \frac{\Delta T}{2} \left[1 - \cos\left(\frac{2\pi x}{L}\right) \right] \quad (1)$$

Each border of the cavity has a length size of L . The temperature reaches its maximum in the top wall centre with a difference of ΔT from the cold two sides imposed to a minimum temperature T_0 . The argon gas used in the study is kept at the environmental temperature $T_0 = 273$. The size of the cavity is $L = 10^{-6}$ m and the applied temperature gradient used to create the non-equilibrium inside the enclosure is $\Delta T = 273K$. The initial density is changed inside the cavity as (Baliti *et al.*, 2017):

$$\rho_0 = \sqrt{\frac{\pi}{2}} \frac{\mu_0}{Kn \sqrt{\theta_0} L} \quad (2)$$

where, $\theta_0 = RT_0$ is the environmental temperature in the energy frame with R is the gas constant, Kn is the Knudsen number and μ_0 is the dynamic viscosity coefficient.

3. SOLUTION METHODS

3.1 DSMC

The direct simulation Monte Carlo method (DSMC) is a molecular-based and statistical method used for the physical simulation of rarefied gases. This method, developed by G. BIRD, is initially used to study the relaxation problems of a homogeneous gas. Then, while improving its algorithm, the use of the method has been extended to systems that operate under low pressure despite of the applications in micro fluidics fields. The DSMC method was validated by comparing with experimental data of rarefied gas flows in the last century (Bird, 1998). It was used to simulate the gas-microflows or the gas flows under low pressure condition (Baliti *et al.*, 2018b; Hssikou *et al.* 2016b). The fundamental approximation of this method lies in molecular chaos and a rarefied gas, where only the binary collisions are considered. So, if the computational time step is smaller than the physical collision time the free motion of the particles, followed by the interactions with the walls, is uncoupled with the intermolecular collisions. This stochastic method treats intermolecular collisions as instantaneous and probabilistic events. The power of the DSMC method lies in the modelling of the gas flow by a limited number of molecules, a few million molecules (Bird, 1994). The positions and velocities of all test particles are generated randomly in cells using the sequences of the pseudo-random numbers. They are stored in the computer and then updated after each time step. In each cell, a certain number of collision pairs are selected using the Bernoulli trials (BT) (Saadati *et al.* 2015; Goshayeshi *et al.* 2015; Roohi & Stefanov, 2016) scheme, which allows the use of a small average number of particles in each cell and avoids repeated collisions, and the calculation of these collisions. The maximum number of collisions N_C in each cell is estimated according to (Bird, 1994; Roohi & Stefanov, 2016):

$$N_C = \frac{1}{2} \frac{N(N-1)F_{eff}(\sigma_{cr})_{max} \Delta t}{V_c} \quad (3)$$

where, N is the number of particles in cell, F_{eff} is the number of real particles represented by a particle simulator, $(\sigma_{cr})_{max}$ is the maximum value of the product of the collision cross section and the relative velocity of the particle partners (this quantity is updated throughout the simulation), Δt is the time step, and V_c is the volume of a cell.

To reduce the number of variables to be memorized, it is often more convenient to choose flows with spatial symmetries. A steady-state of flow field is obtained with a sufficiently long simulation time (Liu *et al.* 2007).

Based on the DSMC theory, the macroscopic velocity can be obtained by the statistic laws (Bird, 1994):

$$v_i = \frac{1}{N_i} \sum c_i \quad (4)$$

where, c_i is the particle velocity. The temperature can be obtained in the same way as:

$$\frac{3}{2} kT = \overline{mv^2} - \overline{m\bar{v}}^2 \quad (5)$$

with k the Boltzmann constant and m is the particle mass. Finally, by ignoring the rotational contribution, monatomic gas, the components of heat flux vector can be calculated for an ideal gas as:

$$q_i = \frac{1}{2} \overline{\rho v^2 v_i} \quad (6)$$

where ρ is the gas density.

3.2 NSF

From hydrodynamic theory of Navier-Stokes and Fourier, balance equations of mass, momentum and energy and relations of stress and heat flux can be written, respectively, as (Struchtrup, 2005; Baliti *et al.* 2016):

$$\frac{\partial \rho}{\partial t} + \frac{\partial \rho v_k}{\partial x_k} = 0 \quad (7)$$

$$\frac{\partial \rho v_i}{\partial t} + \frac{\partial \rho v_i v_k}{\partial x_k} + \frac{\partial \sigma_{ik}}{\partial x_k} + \frac{\partial \rho \theta}{\partial x_i} = 0 \quad (8)$$

$$\frac{3}{2} \frac{\partial \rho \theta}{\partial t} + \frac{3}{2} \frac{\partial \rho \theta v_k}{\partial x_k} + \frac{\partial q_k}{\partial x_k} + \rho \theta \frac{\partial v_k}{\partial x_k} + \sigma_{ik} \frac{\partial v_i}{\partial x_k} = 0 \quad (9)$$

$$q_i = -\frac{15}{4} \mu \frac{\partial \theta}{\partial x_i} \quad (10)$$

$$\sigma_{ij} = -2\mu \frac{\partial v_i}{\partial x_j} \quad (11)$$

The indices inside angular brackets denote the symmetric trace-free part of tensors. The NSF equations are solved numerically with second order of velocity slip and temperature jump boundary

conditions (Gad-el-Hak, 2001; Baliti at al. 2016) using finite difference scheme. The present DSMC simulations and NSF solutions are given to the Maxwell molecules model.

The set of boundary conditions used in the NSF solution are:

$$\sigma_{\tau n} = -\alpha / (2 - \alpha) \left(p v_{\tau} - \frac{3}{4} \mu \frac{\partial \theta}{\partial x_{\tau}} \right) \quad (12)$$

$$q_n = -\alpha / (2 - \alpha) \left(2p(\theta - \theta^w) - \frac{1}{2} p v_{\tau}^2 - \mu \theta \frac{\partial v_n}{\partial x_n} \right) \quad (13)$$

where θ^w is the temperature of the wall. The parameter α is the Maxwell accommodation coefficient which the value is $\alpha = 1$ for the full diffuse reflection and $\alpha = 0$ for the specular one.

The results will be presented in normalized form to the state reference of the equilibrium defined as:

$$x'_i = \frac{x}{W}, \quad T' = \frac{\theta}{\theta_0}, \quad \rho' = \frac{\rho}{\rho_0}, \quad v'_i = \frac{v_i}{\sqrt{\theta_0}},$$

$$q'_i = \frac{q_i}{\rho_0 \sqrt{\theta_0}^3} \quad \text{and} \quad \sigma'_{ij} = \frac{\sigma_{ij}}{\rho_0 \theta_0}. \quad (14)$$

The apostrophe refers to the non-dimensional parameters, and will be dropped in the rest of the paper.

3.3 Validation and Results Accuracy

The present DSMC simulation is adapted to compute the flow characteristics for a microcavity-flow uniformly heated at the bottom side. Well-established results computed by Rana *et al.* (Rana *et al.*, 2015) exist for the same problem which is used for the present simulation-validation exercise. Figure 2 shows the normal heat flux component of the along the centreline (a) and bottom-wall of the cavity (b) for $Kn=0.05$. The agreement between our DSMC results and those of (Rana *et al.*, 2015) is good. The close agreement gives credibility to the result of the simulation, and it stands validated. The results accuracy of the present study (case1) is tested through the mesh grid independence for both DSMC and NSF solutions for the number of cells/nodes $N=10, 30, 50, 100$ (see Table1.). The dimensionless relative error of the temperature is calculated in comparison to its averaged value along the bottom (cold) wall given by: $\bar{\theta} = 1/N \sum_{i=1}^N \theta_{x,0}$. The results confirm that the accuracy depends well on the domain discretisation size. While conserving the computational time, the choice of 100×100 discretisation is proved by the current validation test which that the accuracy of results is enough satisfied.

The time step Δt is also a critical factor in DSMC method. The table 1. shows that the temperature relative error obtained for $\Delta t = 0.1t_c, 0.3t_c, 0.5t_c, 0.7t_c, 1t_c$, with t_c is the collision mean time,

remains close to the 0.03% value. The mass of an argon atom, used in the study, is 6.63×10^{-26} kg and its atomic diameter is 4.17×10^{-10} m (Moghadam *et al.*, 2014; Rabani *et al.* 2018).

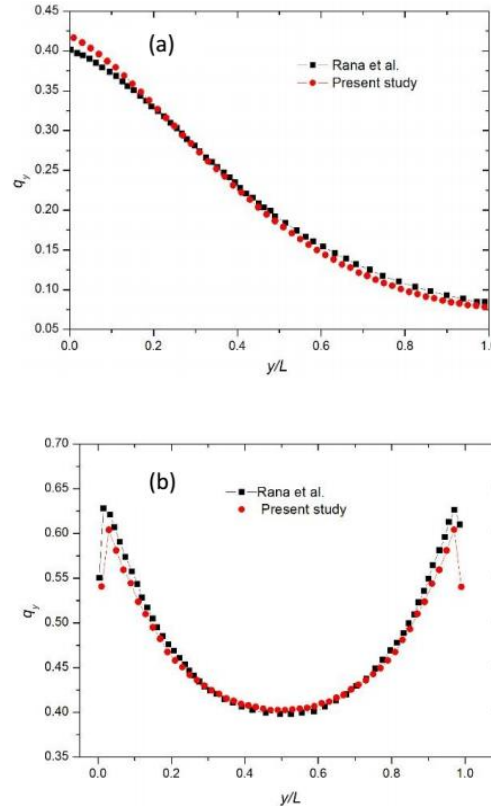


Fig.2. Comparison of the normal heat flux component q_y along the cavity centreline (a) and the heated bottom-wall (b) obtained using the present DSMC and those of Rana *et al.* (Rana *et al.*, 2015) for $Kn = 0.05$.

4. RESULTS

In this study we focus on numerical investigation of rarefaction effects on gas confined within a two-dimensional, rectangular enclosure with a sinusoidal temperature profile imposed at the upper-wall. The applied sinusoidal temperature is symmetric with respect to the midline of the enclosure. The gas flow inside the enclosure is studied using the direct simulation Monte Carlo method for $Kn = 0.05, Kn = 0.1, Kn = 0.3, Kn = 1$ and $Kn = 5$.

The high gradient of temperature taken in hole of study is $\Delta T = 1$. The DSMC results are compared with the Navier-Stokes-Fourier equation, with second order of velocity slip and temperature jump solutions.

4.1 DSMC Description

4.1.1 Case 1

When the rarefied gas effect is considered, the flow

Table 1 Temperature relative error along the microcavity bottom-wall (case 1) obtained using the present DSMC and NSF solutions for $Kn = 0.05$.

	Number of cells/nodes				Time step				
	10	30	50	100	0.1*tc	0.3tc	0.5*tc	0.7*tc	1*tc
DSMC	0.102%	0.046%	0.032%	0.021%	0.0322%	0.0322%	0.0318%	0.0313%	0.0311%
NSF	0.018%	0.012%	0.009%	0.007%	---				

will be induced by the sinusoidal temperature distribution. If the external force is ignored according to the classical non-slip continuum theory, the flow should be absent, and the heat transfer is pure heat conduction (Liu *et al.* 2007). Figure 3 shows the velocity streamlines and the temperature contours for different values of the Knudsen number for results obtained using the DSMC method. Owing to the symmetry in the temperature field, the velocity streamlines are also symmetrical with respect to the midplane ($x = 0.5$). Two remarkable vortices are observed near the heated surface, along the vertical axes, induced by the components of the velocity having a maximum value less than 0.015, equivalent to 5m/s. These eddies are being located near the two upper corners for $Kn=0.05$. The vortex center is located at $x=0.267$ and $y=0.855$. This primary eddy is flowing from the hot regions to cold ones. The temperature contours are thermally stratified due to the conduction which induces the heat transfer inside the cavity. Increasing the Knudsen number, the temperature jump becomes significant and the cavity inside becomes less heated, while the stratification is existent in all Knudsen number values. The growth of the Knudsen number to $Kn=0.1$ allows the creation of the secondary eddies next the lateral walls. These vortices are flowing counter wise from cold to hot regions. From $Kn=1$ to above, another vortices type is created near the two bottom corners. These last eddies are in the same rotation direction as the primary vortices.

The primary vortex center position has no significant change due to the rarefaction. The secondary and third vortices are locating in position ($x=0.077$ and $y=0.121$) and ($x=0.022$ and $y=0.022$) respectively. With the Knudsen number increase, all gradients inside the cavity become less steep. Consequently, the secondary and third eddies becomes more pronounced. The formation of primary vortices is induced by the tangential temperature gradient in the gas near the vertical surface that forces a creep-driven fluid into a circulatory motion (Baliti *et al.* 2016; Rana *et al.*, 2012). The secondary counter rotating recirculations in the two lateral sides are due to the competition between the viscous and transpiration part of the tangential velocity, where the dominance is in favor of the stress for high Knudsen numbers (Baliti *et al.* 2016; Rana *et al.* 2012). The third vortices type near bottom corners is created by distortion of the primary eddies by secondary ones, creating from the two rotating vortices four ones flowing in the same direction. The

secondary vortices become bigger at the expense of the primary distorted ones.

4.1.2 Case 2

The main characteristics of heat conduction in the present enclosure with the upper wall subjected to a sinusoidal temperature distribution are shown in Figure 4. The flow and temperature fields are presented in terms of streamlines and isotherms of the second case, where the three walls are adiabatic, for five Knudsen number values 0.05, 0.1, 0.3, 1 and 5 and a temperature gradient of $\Delta T = 1$. These plots show that, due to the symmetric boundary condition at the upper wall together with the adiabatic conditions on the side and bottom walls, both the flow and temperature fields are symmetric about the midline of the enclosure.

A pair of identical counter-rotating vortices is formed in the left and right halves of the enclosure. The gas moves horizontally from the hotter middle of the upper wall toward its colder edge; then it descends along the adiabatic cooler sidewall; and finally, it ascends near the symmetry plane (Sarris *et al.*, 2002). These eddies are as the primary ones in the first case, filling the hole inside of the cavity. The vortex center is located at $x=0.255$ and $y=0.8$. The rarefaction has no effect on the vortices center, which remains in the same position, despite the Knudsen number increase. The temperature fronts penetrate from the upper wall deep inside the gas body as conduction is the main heat transfer mechanism in this case. As observed in the first case, the temperature in this case decreases with rarefaction increase.

4.1.3 One Dimensional Plot

To make a great understanding of the rarefaction effects, the variations of the horizontal velocity, the vertical heat flux along the sinusoidally heated plate and the temperature distribution along the vertical centerline for both cases are illustrated in Fig.5. The velocity component shows a sinusoidal profile and becomes weakened by the rarefaction increase. The horizontal component of the velocity is quite pronounced in case 2 more than in case 1, which is due to the difference of boundary conditions between them. The y-heat flux presents a parabolic profile in the bulk which is affected in case 1 boundaries for low Knudsen numbers more than the other one. It is very marked in case 2 more than that

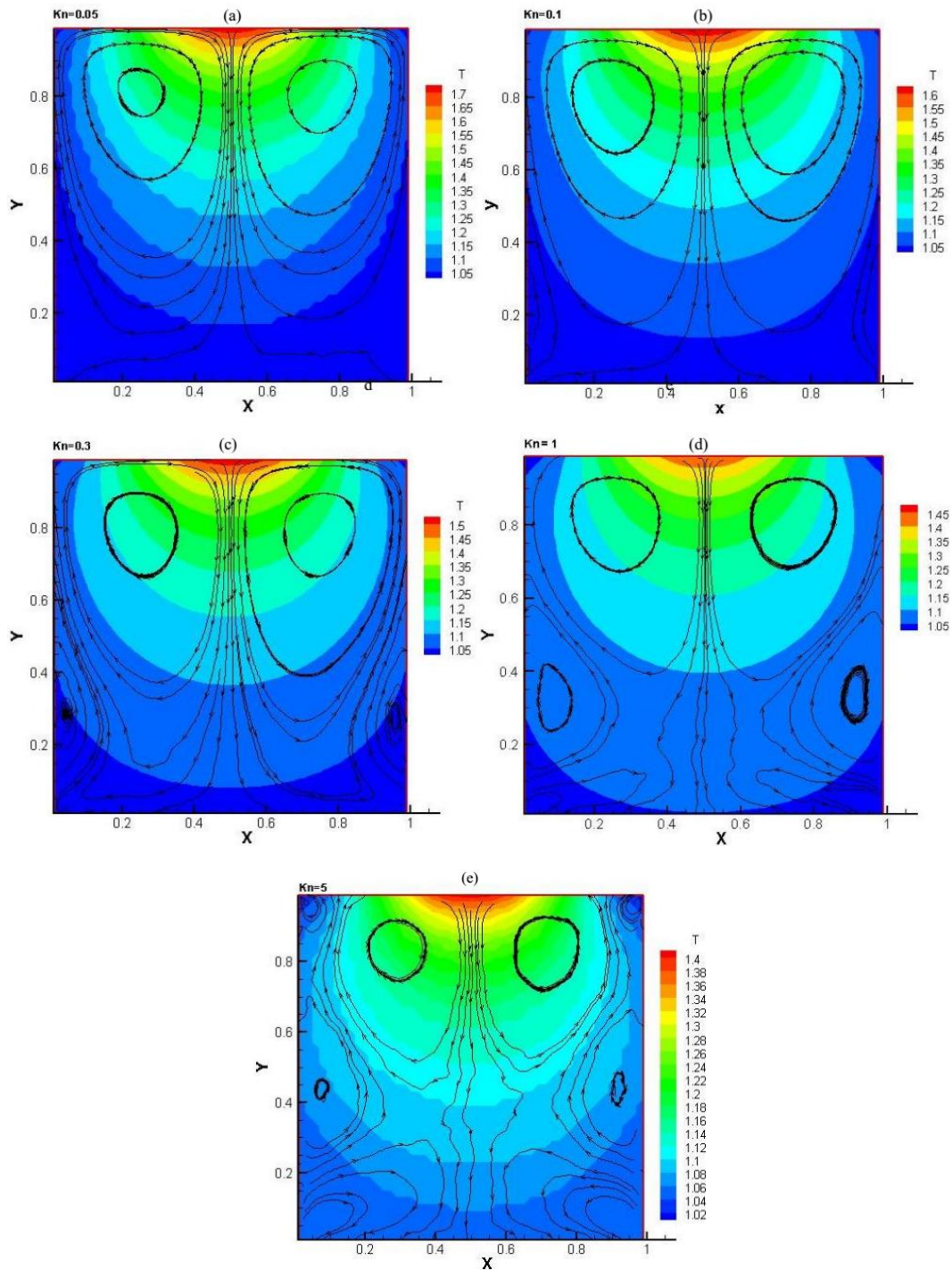


Fig.3. Streamlines and temperature contours for (a) $Kn = 0.05$, (b) $Kn = 0.1$, (c) $Kn = 0.3$, (d) $Kn = 1$ and (e) $Kn = 5$ using the DSMC method (case 1).

calculated from with fully diffuse boundary conditions. To analyze the reason of the vertical heat flux, decrease by the rarefaction, the temperature is plotted for the two cases in Fig.5c, which shows that the rarefaction greatly decreases the temperature gradient near the surfaces (Liu *et al.* 2007).

4.2 Comparison with NSF Model

It is generally regarded that the NSF model, solved

using various velocity slip and temperature-jump boundary conditions, can capture some flow features rather in the slip regime. However, in certain instances, the NSF model does not capture several well-known nonequilibrium phenomena such as the bimodal temperature profile in force-driven Poiseuille flow (Mansour *et al.* 1997) and non-gradient heat flux in Couette flow (Gu & Emerson, 2009). This study has been realized to test whether the NSF model, modified with second

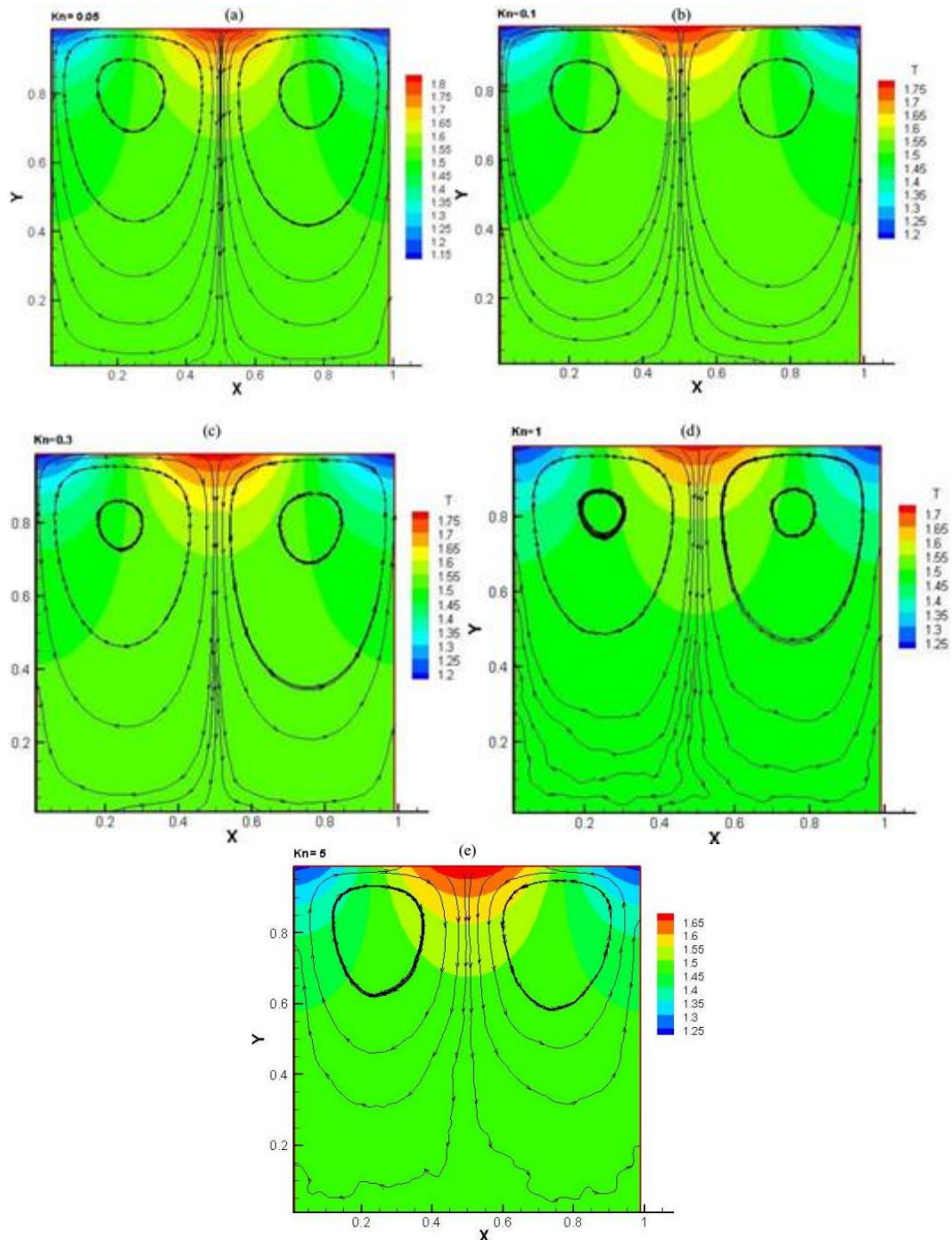


Fig.4. Streamlines and temperature contours for (a)Kn=0.05, (b)Kn=0.1, (c)Kn=0.3, (d)Kn=1 and (e)Kn=5 using the DSMC method (case 2).

order velocity slip and temperature jump boundary conditions, can capture critical flow features accurately in the slip regime for the heat transfer within the cavity with sinusoidal temperature at the top wall for the two cases of different type of boundary conditions.

4.2.1 Case 1

Figure 6 illustrates the velocity streamlines and temperature contours obtained by the NSF solutions for the Knudsen number $Kn=0.05$ and 0.1 with a

temperature gradient $\Delta T=1$, for the case 1. The plots show that there is only one vortices kind in the cavity which is the same as predicted by the DSMC method (Fig.3). The vortices center is displaced compared with the DSMC prediction to the top corners to the position $x=0.244$ and $y=0.867$. The temperature contour demonstrates that the conduction is the main mechanism for heat transfer inside the cavity. But the temperature jump seems very important especially from the heated wall.

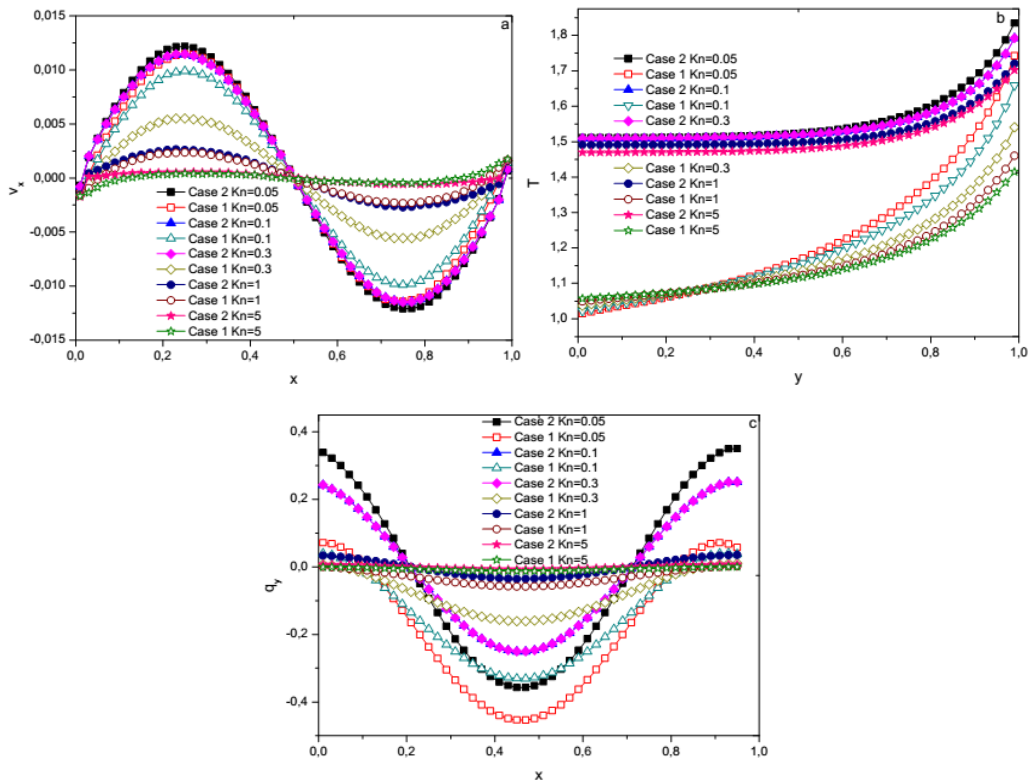


Fig.5. (a) x- component of velocity,(b)y- component of heat flux about the heated plate and (c)temperature along the vertical centerline for both cases.

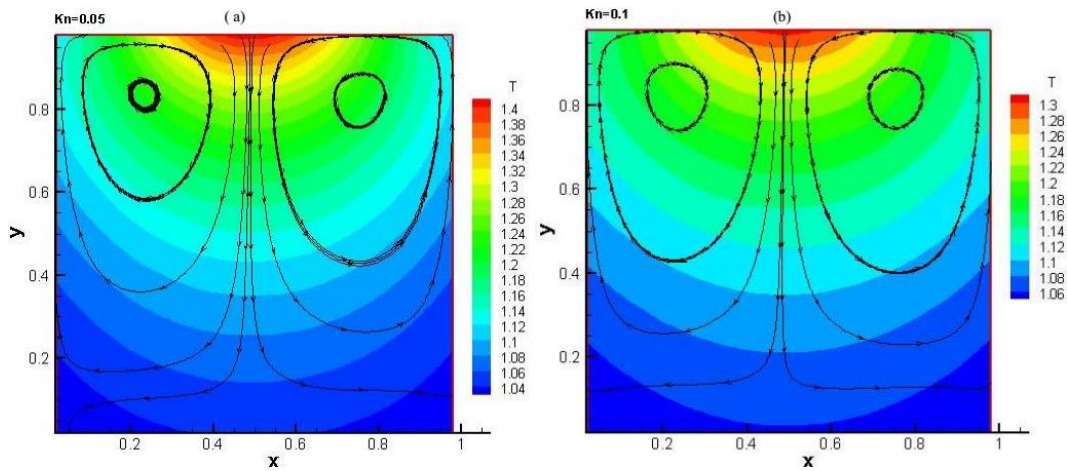


Fig.6. Streamlines and temperature contours for (a) $Kn = 0.05$ and (b) $Kn = 0.1$, using th NSF solutions (case 1).

4.2.2 Case 2

Streamlines overlaid on the temperature contours are plotted in fig.7, for Knudsen values 0.05 and 0.1 for the case with three adiabatic walls and a temperature gradient $\Delta T = 1$. The symmetricity of streamlines and temperature contours is observed. The classical vortices are predicted as in Fig.4. Their centers are shifted slightly to the top plate, in comparison to DSMC solutions, to reach the position $x=0.255$ and $y=0.872$. The conduction leads the hot temperature front to permeate from the upper wall center deep

inside the gas body.

4.2.3 Macroscopic Parameters Plots.

Figure 8 shows the horizontal velocity component, vertical heat flux along the sinusoidally heated plate and temperature profile along the vertical centerline for $Kn=0.05$ predicted by both used method for two cases. As the flow goes far from the thermodynamic equilibrium by the temperature gradient, the vertical heat flux cannot be predicted by the well-known second order approximation. Although horizontal velocity component profile along the heated plate is

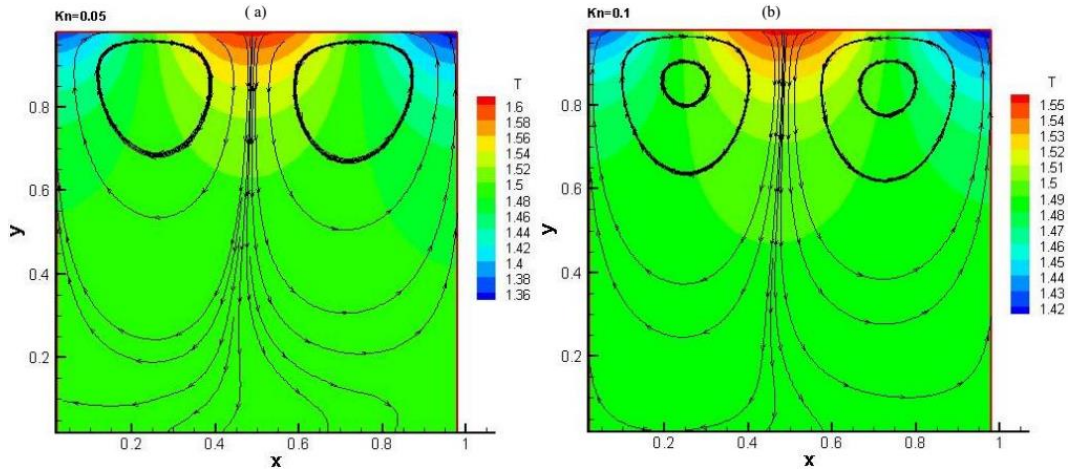


Fig.7. Streamlines and temperature contours for (a) $Kn = 0.05$ and (b) $Kn = 0.1$, using th NSF solutions (case 2).

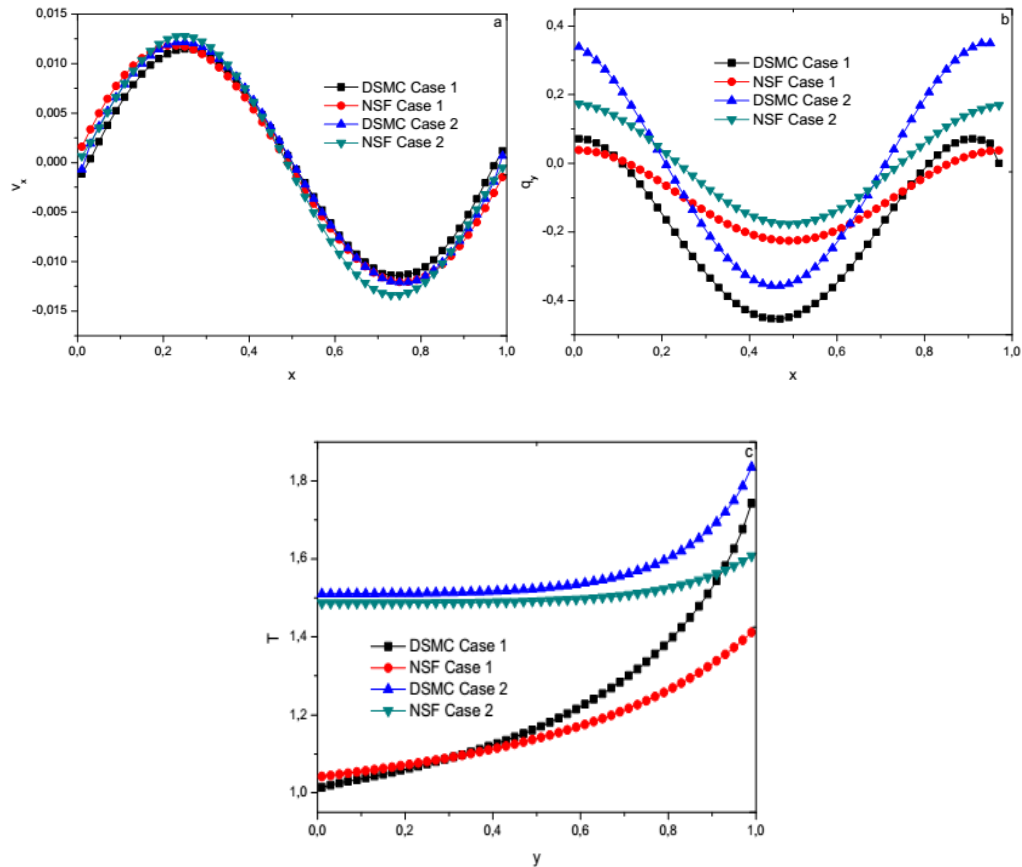


Fig. 8. (a) x- component of velocity,(b)y- component of heat flux about the heated plate and (c)temperature along the vertical centerline for both cases predicted by NSF and DSMC for $Kn=0.05$.

predicted quite correctly with the velocity slip and temperature jump boundary condition, heat flux cannot be predicted in the non-equilibrium regions. Furthermore, y-heat flux contour about the upper wall of the cavity is quite different from the predicted results of the continuum approach.

According to the molecular relations, heat flux is obtained by the Eq. (6), while NSF equations yield

the simple constitutive Fourier relation for heat flux (equation (10)) which do not take into account the shear stress effect in heat transfer. The heat flux predicted by the continuum-based solution is lower than that obtained by DSMC. The reason is illustrated by Fig.8d which is showing that the temperature in NSF is greatly decreased near the surfaces compared to that in DSMC. As a

consequence, the heat flux is enhanced in DSMC, while it is weakened in NSF by the temperature by the fact that it does not take into account the flow effect.

If we compare the temperature of the two cases (Fig.5b), we can observe the effect of thermalized walls in comparison with adiabatic ones. Where, the effect of cold walls increases the coolness inside the cavity especially with the Knudsen number increase. That is due to the wall force (Rabani *et al.*, 2018) which is not treated here in comparison with the molecular dynamic simulation. This nonideal behavior of a gas, encountered more at the nanoscale size, affects the heat transfer process by means of skin friction that acts as a wall force field thermal resistance (Rabani *et al.*, 2018). To capture that effects in DSMC calculation of heat transfer, the equation (6) should be modified according to the Van der Waals equation of state (Wang *et al.*, 2003). Using the dynamic molecular approach, Rabani *et al.* show that the wall force field forms a considerable part of the total thermal resistance (approximately 20% of total thermal resistance for 540nm height channel) of the rarefied gas medium.

5. CONCLUSION

The heat transfer within a square cavity with heated upper wall by a sinusoidal temperature is investigated with the direct simulation Monte Carlo. The cavity is taken for two different boundary conditions, where in the first case all walls are diffuse reflecting, while in the other three plates are adiabatic. The results obtained are compared to the based continuum approach with second velocity slip and temperature jump boundary conditions. The essential of the results come out from the study show that in the first case when the Knudsen number is low, two vortices are filling the quasi-totality of the cavity. While, the increase of rarefaction shows two other counter rotating vortices ($Kn=0.3$), which become more extended when the gas become more rarefied ($Kn=1$, and above). The case 2 presents only two eddies in the whole of Knudsen numbers without any affection with rarefaction increase. Good agreement is obtained between the NSF and DSMC model for the horizontal velocity component, as expected in the slip regime near the sinusoidally heated wall. Normal heat flux to the heated wall is enhanced by the flow in DSMC rather than the lower predicted by NSF basing on the Fourier law.

REFERENCES

- Baliti, J., M. Hssikou and M. Alaoui (2016). Numerical simulation of heat transfer in a micro-cavity. *Canadian Journal of Physics* 999, 1-10.
- Baliti, J., M. Hssikou and M. Alaoui (2017). The 13-moments method for heat transfer in gas microflows. *Australian Journal of Mechanical Engineering* 1-14.
- Baliti, J., M. Hssikou and M. Alaoui (2018a). Rarefaction and external force effects on gas microflow in a lid-driven cavity. *Heat Transfer-Asian Research*.
- Baliti, J., M. Hssikou and M. Alaoui (2018b). Monte Carlo simulation of nonlinear gravity driven Poiseuille–Couette flow in a dilute gas. *Monte Carlo Methods and Applications* 24(3), 153-163.
- Beskok, A. (2001). Validation of a new velocity-slip model for separated gas microflows. *Numerical Heat Transfer: Part B: Fundamentals* 40(6), 451-471.
- Bird, G. A. (1994). Molecular gas dynamics and the direct simulation monte Carlo of gas flows. Clarendon Press, Oxford.
- Bird, G. A. (1998). Recent advances and current challenges for DSMC. *Computers & Mathematics with Applications* 35(1-2), 1-14.
- Bird, G. A. (1976). Molecular gas dynamics. Clarendon Press, Oxford University.
- Cercignani, C. and E. Gabetta (2007). Transport phenomena and kinetic theory: applications to gases, semiconductors, photons, and biological systems. Springer Science and Business Media.
- Chapman, S. and T. G. Cowling (1970). The Mathematical Theory of Nonuniform Gases, Cambridge University Press, New York.
- Gad-el-Hak, M. (2001). The MEMS handbook. CRC Press.
- Goshayeshi, B., E. Roohi and S. Stefanov (2015). A novel simplified Bernoulli trials collision scheme in the direct simulation Monte Carlo with intelligence over particle distances. *Physics of Fluids* 27(10), 107104.
- Gu, X. J. and D. R. Emerson (2009). A High-Order Moment Approach for Capturing Non-Equilibrium Phenomena in the Transition Regime. *Journal of Fluid Mechanics* 636, 177–216.
- Hssikou, M., J. Baliti and M. Alaoui (2016b). The planar Couette flow with slip and jump boundary conditions in a microchannel. *Monte Carlo Methods and Applications* 22(4), 337-347.
- Hssikou, M., J. Baliti and M. Alaoui (2016a). Extended macroscopic study of dilute gas flow within a microcavity. *Modelling and Simulation in Engineering*.
- Islam, N. and S. Sayed (2012). MEMS Microfluidics for Lab-on-a-Chip Applications. In *Microelectromechanical Systems and Devices*. InTech.
- Jian, C. Q., A. Dutta, A. Mukhopadhyay and D. P. Tselepidakis (2000). Explicit Coupling Between Combustion Space and Glass Tank Simulations for Complete Furnace Analysis, in Proc. 1st Balkan Conference on Glass Science and Technology, Greece, pp. 402-409, University of Thessaly, Volos.

- Karniadakis, G. E., A. Beskok and N. Aluru (2006). *Microflows and nanoflows: fundamentals and simulation* (Vol. 29). Springer Science & Business Media.
- Le, M. (2006). *DSMC simulation of flows in multiple microchannel geometries* (Doctoral dissertation, Concordia University).
- Liu, H., M. Wang, J. Wang, G. Zhang, H. Liao, R. Huang and X. Zhang (2007). Monte Carlo simulations of gas flow and heat transfer in vacuum packaged MEMS devices. *Applied thermal engineering* 27(2), 323-329.
- Mansour, M. M., F. Baras and A. L. Garcia (1997). On the Validity of Hydrodynamics in Plane Poiseuille Flow. *Physica A* 240, 255-267.
- Moghadam, Y. E., E. Roohi and J. A. Esfahani (2014). Heat transfer and fluid characteristics of rarefied flow in thermal cavities. *Vacuum* 109, 333-340.
- Rabani, R., G. Heidarnejad, J. Harting and E. Shirani (2018). Interplay of confinement and density on the heat transfer characteristics of nanoscale-confined gas. *International Journal of Heat and Mass Transfer* 126, 331-341.
- Rana, A. S., A. Mohammadzadeh and H. Struchtrup (2015). A numerical study of the heat transfer through a rarefied gas confined in a microcavity. *Continuum Mechanics and Thermodynamics* 27(3), 433-446.
- Rana, A., M. Torrilhon and H. Struchtrup (2012). Heat transfer in micro devices packaged in partial vacuum. *Journal of Physics* 362.
- Roohi, E. and S. Stefanov (2016). Collision partner selection schemes in DSMC: From micro/nano flows to hypersonic flows. *Physics Reports* 656, 1-38.
- Saadati, S. A. and E. Roohi (2015). Detailed investigation of flow and thermal field in micro/nano nozzles using Simplified Bernoulli Trial (SBT) collision scheme in DSMC. *Aerospace Science and Technology* 46, 236-255.
- Sarris, I. E., I. Lekakis and N. S. Vlachos (2002). Natural convection in a 2D enclosure with sinusoidal upper wall temperature. *Numerical Heat Transfer: Part A: Applications* 42(5), 513-530.
- Sarris, I. E., N. Katsavos, I. Lekakis and N. S. Vlachos (1999). Modelling the Influence of Combustion on Glass Melt Flow (in Greek), in *Proc. 6th National Conf. of Solar Technology Institute, Greece*, vol. 2, pp. 201-209, University of Thessaly, Volos.
- Struchtrup, H. (2005). *Macroscopic transport equations for rarefied gas flows*. Springer, New York.
- Struchtrup, H. and P. Taheri (2011). Macroscopic transport models for rarefied gas flows: a brief review. *IMA journal of applied mathematics* 76(5), 672-697.
- Wang, M. and Z. Li (2003). Nonideal gas flow and heat transfer in micro-and nanochannels using the direct simulation Monte Carlo method. *Physical Review E* 68(4), 046704.